RELATIONSHIP BETWEEN DAMAGE AND PERMEABILITY IN LINER-LESS COMPOSITE TANKS: EXPERIMENTAL STUDY AT THE LAMINA LEVEL

Hortense Laeuffer[(1,2)] , **Brice Guiot**[(2)] , **Jean-Christophe Wahl**[(2)] , **Nicolas Perry**[(3)] , **Florian Lavelle**[(1)] , **Christophe Bois**[(2)]

[(1)] *CNES, 52 rue Jacques Hillairet 75612 Paris, France, +33 5 56 84 79 76,*
hortense.laeuffer@u-bordeaux.fr
[(2)]*Univ. Bordeaux, I2M, UMR 5295, F-33400 Talence, France,*
IUT de Bordeaux 15 rue Naudet 33175 Gradignan, christophe.bois@u-bordeaux.fr
[(3)]*Arts et Metiers ParisTech, I2M, UMR 5295, F-33400 Talence, France,*
Esplanade des Arts et Metiers, 33405 Talence, France, nicolas.perry@ensam.eu

ABSTRACT

The aim of this study is to provide a relevant description of damage growth and the resultant crack network to predict leaks in liner-less composite vessels. Tensile tests were carried out on three different laminates: $[0_2/90_n/0_2]$, $[+45/-45]_{2s}$ and $[0/+67.5/-67.5]_s$. Number n varies from 1 to 3 in order to study the effect of ply thickness. Transverse crack and delamination at crack tips were identified with an optical microscope during tensile loading. A length of 100 mm was observed for several loading levels to evaluate statistical effects. Results highlight a preliminary step in the damage scenario with small crack densities before a second step where the crack growth speeds up. In bulk, cross-section examinations showed that no delamination occurred at crack tip in the material of the study (M21 T700). Cross-section examinations were also performed on $[+45/-45]_{2s}$ and $[0/+67.5/-67.5]_s$ layups in order to bypass the issue of free edge effects. Damage state in those layups was shown to be significantly different in the bulk than at the surface. Observations of the damage state in bulk for those layups demonstrated that there is no transverse crack in $[+45/-45]_{2s}$ specimens subjected to shear strains up to 4%, and that interactions between damage of consecutive plies strongly impact both the damage kinetics and the arrangement of cracks. These elements are fundamental for the assessment of permeability performance, and will be introduced in the predictive model.

1. INTRODUCTION

Designing liner-less composite vessels for launch vehicles enables to save both cost and weight. Therefore, this is a core issue for aerospace industry. In usual composite vessels, the liner is a metallic or polymer part in charge of the gas barrier function. One challenge when designing a liner-less vessel is to reach the permeability requirement with the composite wall itself. Pristine composite laminates meet the permeability requirement, but as those materials are heterogeneous, damage growth may occur in cases of low thermo-mechanical loads. Transverse cracks and micro-delamination in adjacent plies grow and may connect together (Fig. 1), resulting in a leakage network through the composite wall.

On the ply scale, transverse cracks are generated by transverse stress (mode I) and shear stress (mode II). Developing a model that predicts damage densities and arrangement for any laminate
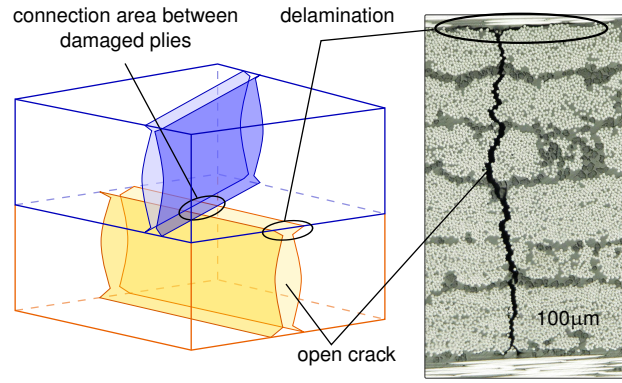
Fig. 1. Transverse crack and delamination : crack network in two damaged plies and micrograph of one transverse crack with delamination at crack tip.

requires reliable experimental data for both modes. The aim of this study is to provide a relevant description of damage growth and the resultant network to predict leaks.

The first part of this experimental study describes the method for damage characterisation. The second part presents the results obtained on the evolution of damage densities. Finally, the third part is devoted to the morphology of the damage network.

2. METHOD FOR DAMAGE CHARACTERISATION

2.1. Damage description

The meso-damage state of each ply of a laminate can be described by two damage densities, as illustrated in Fig. 2: the crack density ρ, which is the average number of transverse cracks over the observed length L, and the micro-delamination length μ, which is the average length of micro-delamination at each crack tip. The corresponding dimensionless variables are defined by:

the crack rate :
$$\bar{\rho} = \rho h = \frac{N}{L} h \tag{1}$$

the delamination rate :
$$\bar{\mu} = \mu \rho = \mu \frac{N}{L} \tag{2}$$

where h denotes the ply thickness and N the number of cracks observed on the length L. Crack and micro-delamination rates are average variables, so that the damage stage is considered homogeneous in each ply. When used as damage variables in a model, the damage densities define the crack pattern which is commonly considered as periodic [1]. Experimental values and evolution of damage densities can be obtained by observation by optical microscopy [2–4] or X-ray tomography as well.

2.2. Instrumentation and method

Transverse cracks are generated by transverse stress (mode I) and shear stress (mode II). This requires testing different laminates in order to characterise damage growth in the ply in both modes or in mixed mode I + II. In this study, three different laminates were tested: $[0_2/90_n/0_2]$, $[+45/-45]_{2s}$ and $[0/+67.5/-67.5]_s$. The effect of ply thickness is also studied by making number n vary from 1 to 3.
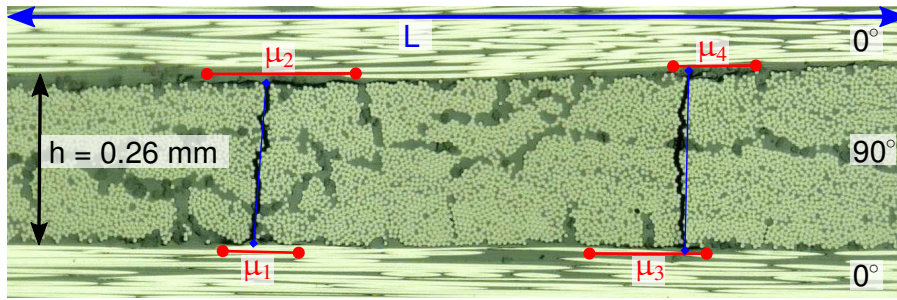
Fig. 2. Measurement of the crack density ρ and average delamination at crack tip μ in a $[0_2/90/0_2]$ lay-up.

In the present work, the assessment of the damage densities was carried out by optical microscopy for several loading levels. Tensile test were performed on specimens polished on one edge. Transverse crack and delamination at crack tips were identified with a travelling optical microscope (Fig. 3). The observation area was chosen quite large, i.e. about 100 mm, in order to evaluate statistical effects. The material is carbon fibre and thermoset matrix M21 T700. Plate samples were manufactured by Automated Fibre Placement (AFP). The thickness of the elementary layer is 0.26 mm. Several layers of the same orientation can be stacked together in order to obtain a thicker ply, e.g. in a $[0_2/90_3/0_2]$ laminate the thickness of the $90°$ ply is 0.78 mm.
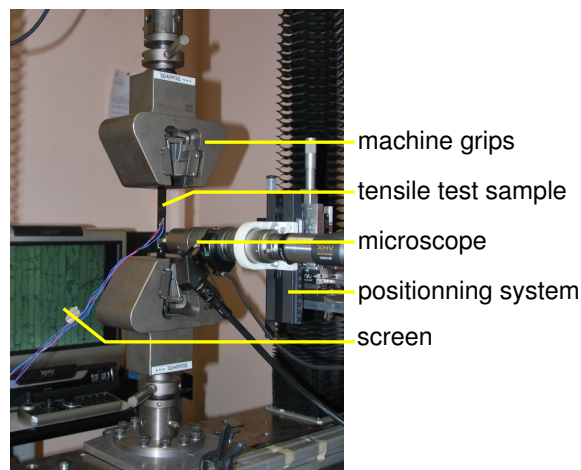
Fig. 3. Damage observation under tensile loading test.

A specific protocol was applied in order to bypass the issue of free edge effects. Observation of the surface under loading was combined to cross-section examination : polishing of the edge was performed after loading in order to remove from 15 μm to 2 mm of the edge surface and observe the damage state in bulk. After polishing, the sample was loaded to a lower level so that damage did not propagate but cracks opened and became more easy to distinguish. Those steps were repeated for increasing maximal loading to obtain the evolution laws of damage in bulk. Beside crack growth characterisation, performing several cross-section examinations through the width of a specimen also allows to study the arrangement of cracks in three dimensions.

3. EVOLUTION OF DAMAGE DENSITIES

3.1. Edge effects

Cross section examinations were carried out on damaged tensile test specimens of $[0_2/90_n/0_2]$ and $[+45/-45]_{2s}$ layups. Measurements were performed on representative areas of about 50 mm long. Fig. 4 shows a transverse crack and the associated micro-delamination at crack tips on the edge of the sample before and after removing 15 microns by a polishing procedure. 15 microns under the edge surface, no visible delamination remains. Fig. 5(a) presents the evolution of micro-delamination rates before and after polishing for three ply thicknesses. Independently of the ply thickness, the micro-delamination rate tends quickly to zero. Cross section examinations were continued to verify the length of cracks. The crack rate with respect to the polishing depth is reported in Fig. 5(b). Cracks were shown to be continuous for double and triple 90 plies, while a few cracks disappeared in the $[0_2/90_1/0_2]$ lay-up. This is consistent with edge effects in this layup. This variation of crack rate for the simple ply is about 15% of the crack rate at the surface (see Fig. 6).
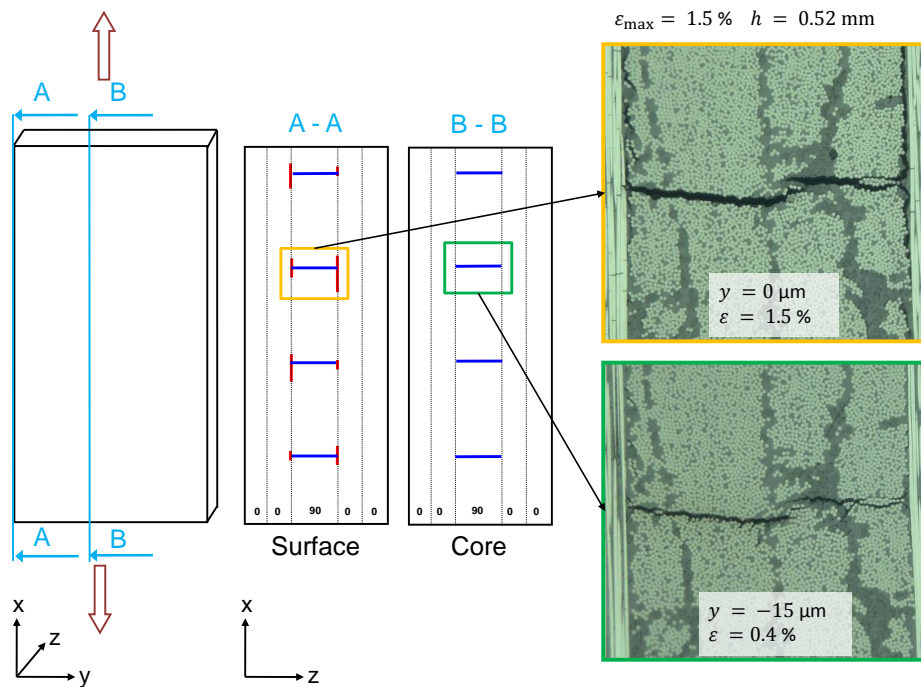

Fig. 4. Cross-section examinations on $[0_2/90_2/0_2]$: diagram of the cross-sections and micrographs at the surface ($y = 0\mu$m) and after removing 15 microns ($y = 15\mu$m).

The $[+45/-45]_{2s}$ layup was subjected to transverse strains up to $\varepsilon_{12} = 4\%$, polished and then observed. For the highest strain and after removing 1.5 mm, only a few transverse cracks remained in the central (and double) ply and in external plies. Deeper, after removing 3 mm of the surface, no crack remained at all. To exclude the eventuality of cracks being too closed to be observable, the sample was observed under loading. The results demonstrates that no transverse cracks nor micro-delamination occur in the bulk under shear load. This phenomenon can be due to the use of a toughened matrix (M21) with thermoplastic nodules. For another material, e.g. with a more fragile matrix, delamination would likely be lower in bulk than at the surface but may persist in bulk. Although no meso-damage is observable, this layup nevertheless undergoes irreversible strains and stiffness loss due to diffuse damage at the micro (fibre) scale. However, if shear loading alone does not lead to transverse cracking in this material, the shear component associated to a tensile loading will likely contribute to crack growth. This contribution may require additional testing on other layups.

(a) Delamination rate $\bar{\mu}$ vs polishing depth.
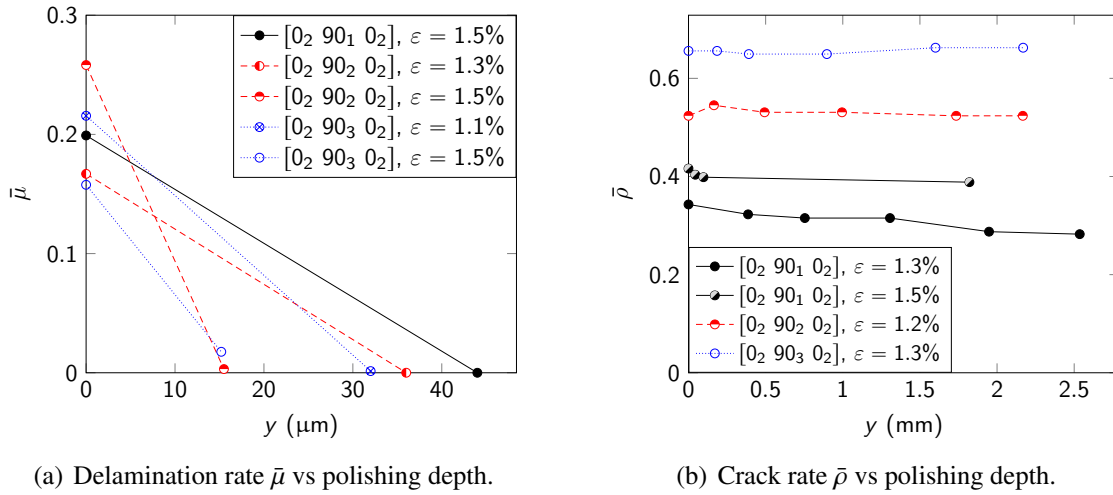
(b) Crack rate $\bar{\rho}$ vs polishing depth.

Fig. 5. Damage rates with respect to the polishing depth y after the transverse strain ε was applied.
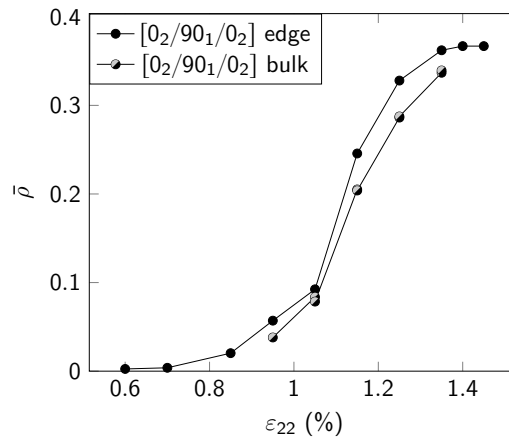

Fig. 6. Crack rate $\bar{\rho}$ with respect to the transverse strain ε_{22} at the surface of the edge and in bulk.

3.2. Evolution of transverse cracking

Evolution of transverse cracking was observed as previously described in Section 2.2 for $[+45/-45]_{2s}$ and $[0_2/90_n/0_2]$ layups with n varying from 1 to 3. As the first one was shown to be not subjected to transverse cracking, this section is devoted to the latter. The position of cracks measured for several loading levels on a $[0_2/90_1/0_2]$ specimen is plotted in Fig. 7(a). The corresponding crack rate has been computed for the whole observed area and also for each separate third of the same area, see Fig. 7(b). The two figures highlight the benefit of observing a large enough and hence representative area. Depending on the piece of sample one chose to focus on, initiation and slope of crack growth may be very different, at least concerning the beginning of crack growth. It is likely due to weak areas (defect locations) that drive the position of the first cracks. The effect of defects on the damage threshold vanishes when damage increases: for higher strains, the distance between consecutive cracks becomes more homogeneous, and no major difference can be observed between the three small areas. The average crack rate computed on the whole length reveals a preliminary step with a progressive beginning of cracking.

The evolution of damage densities according to the applied strain for two ply-thicknesses are presented in Fig. 8. In all cases, the preliminary step in the damage scenario with small cracking rates before a second step where the crack growth speeds up was observed. The curves shows an increase in cracking threshold when the ply thickness decreases. This phenomenon is explained by the energy
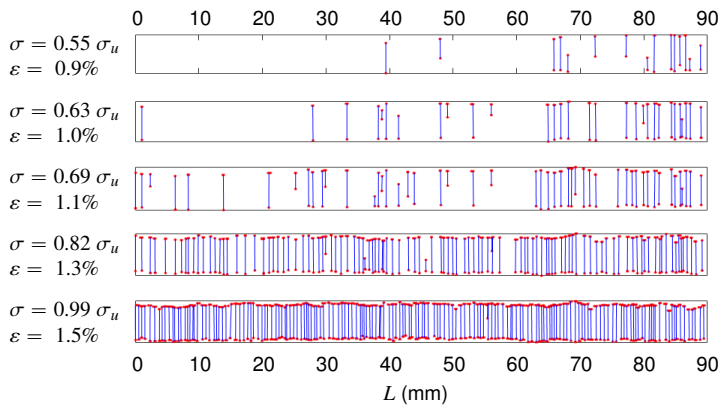
(a) Position of cracks observed on the edge for 5 loading levels.
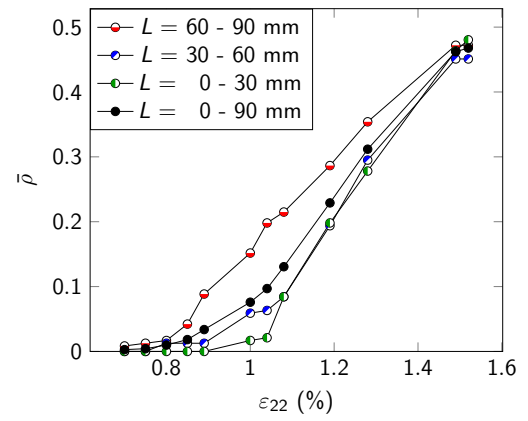
(b) Crack density $\bar{\rho}$ at the surface.

Fig. 7. Damage measurements on a $[0_2/90_1/0_2]$ specimen, ply thickness $h_{90} = 0.26$ mm.

released by the fracture being lower for a thinner ply. This point is widely described in the literature [5–7] and obviously makes thin ply very competitive for liner-less composite vessel.
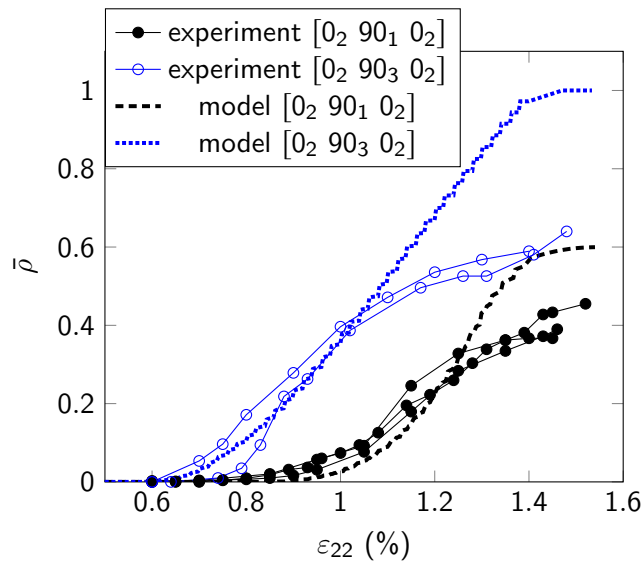

Fig. 8. Measured and predicted crack rates.

The modelling of the preliminary step is fundamental for the prediction of first leak path. This phenomenon due to the variability of the material properties can be introduced in the damage model through a probabilistic approach [8]. Evolution laws for transverse cracks and micro-delamination were built based on Finite Fracture Mechanics and energy release rates [9, 10]. Probability density functions are defined for fracture toughness and strength threshold. A set of simulations are then performed and the average response of the model are computed according to the weight associated to the density functions. Results of the simulation for both ply thicknesses are presented in Fig. 8 by doted and dashed lines. Preliminary step in the damage scenario is well described even though the densities of probability were not accurately identified yet.

4. MORPHOLOGY OF THE DAMAGE NETWORK

To study the shape of a damage network, damage observation under loading and cross-section examination were applied to $[0/+67.5/-67.5]_s$ specimens. The interest of this lay-up is that transverse

cracking can occur in three different and consecutive plies, leading to the creation of a network. The results presented here concern one damage network (without damage growth) observed at several polishing depth from 0.2mm to 5mm.

At the scale of the specimen, the results provide an overview of the network. The position of cracks is schematically drawn in Fig. 9 from the observations. The centre ply, $-67.5°$, is also a double ply, and thus has a lower cracking threshold. In this ply, cracks occurred first and were continuous through the width. Conversely, cracks in the simple $+67.5°$ plies were short and located around the cracks of the double ply. Hence, existence of cracks in an adjacent ply drives the position and the length of the new cracks. Moreover, the cracking threshold of the simple plies is also modified: cracks occur almost simultaneously in the three plies despite their different thicknesses. Tests on $[0/+67.5/0/67.5]_s$ specimens in which cracked plies are isolated are scheduled. Comparing the results obtained with isolated and not-isolated plies will make it possible to quantify the effect of the interaction between cracks in adjacent plies.
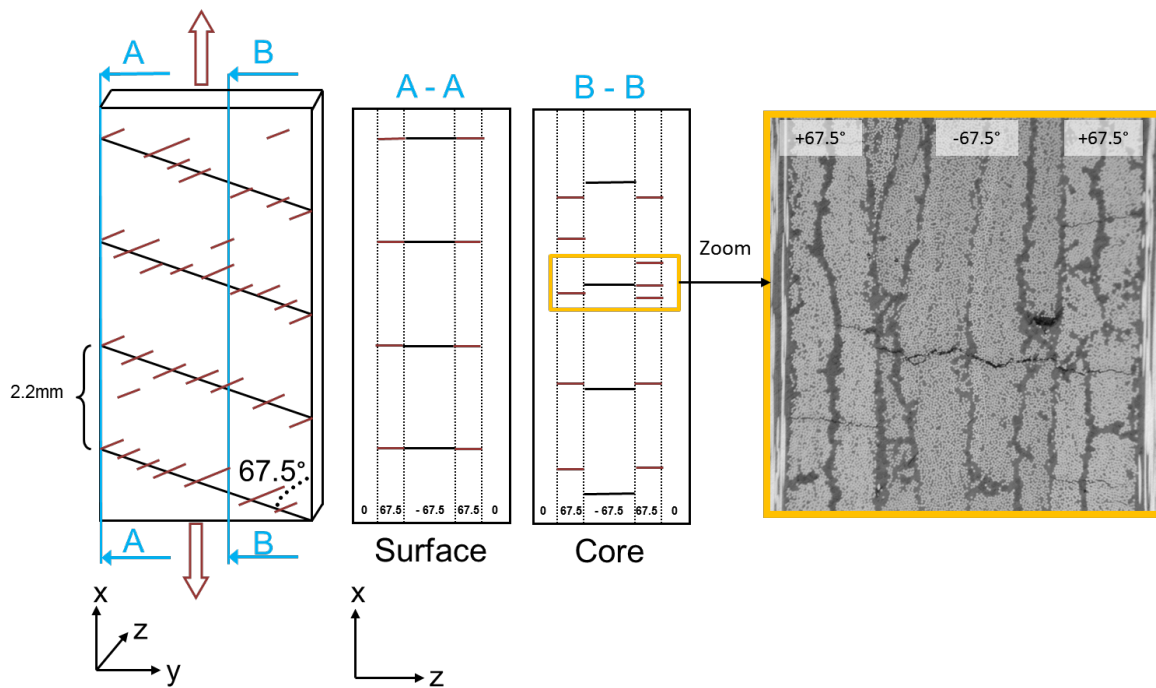

Fig. 9. Crack network in a $[0/+67.5/-67.5]_s$: diagram of the network and micrograph of the three damaged plies.

Fig. 10 focuses on the intersection of three cracks. At the interface between two plies, delamination connects the cracks. This makes the connection area larger than the Crack Opening Displacement (COD) at crack tip and may increase the leakage rate induced by a leak path.

5. CONCLUSION

Transverse crack and delamination at crack tips were identified with an optical microscope during tensile loading. A length of 100 mm was observed for several loading levels. This allowed to highlight a preliminary step in the damage scenario with small crack densities and progressive growth before a second step with a steeper growth. In bulk, cross-section examinations showed that no delamination occurred at crack tip in the material of the study. Cross-section examinations were also performed for
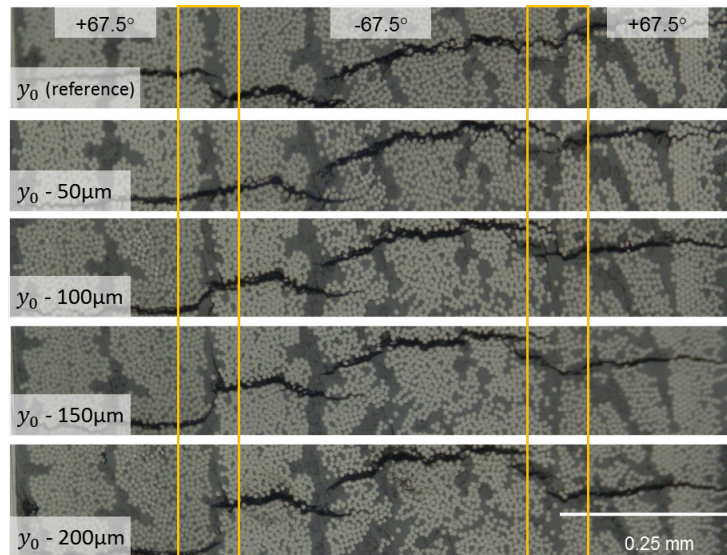
Fig. 10. Intersection between the cracks of three plies in a $[0/+67.5/-67.5]_s$ for several polishing depth.

the observation of $[+45/-45]_{2s}$ and $[0/+67.5/-67.5]_s$ layups in order to bypass the issue of free edge effects. Damage state in those layups was shown to be significantly different through the width of the specimens than at the surface of the edges. Particularly, there is no transverse crack in $[+45/-45]_{2s}$ specimens subjected to shear strains up to 4%. It was also observed that crack growth and crack length are modified by the damage state of adjacent plies. These elements are fundamental for the assessment of permeability performance, and thus will be introduced in the model.

Predicting the percolation of the network also requires to describe the network in terms of number of connections between two adjacent plies. It could be achieved by using only crack density and ply angle, but this is not trivial any more since crack growth and crack length are modified by the damage state of neighbouring plies. Cross-section examinations give an insight into the network pattern, nevertheless this method is restrictive because it is destructive, not very accurate and time-consuming. Additional experiments involving X-ray tomography are required to accurately characterise the crack network pattern. This kind of experiment remains a challenge because of the mismatch between the size of the crack pattern (3mm in the case of the $[0/+67.5/-67.5]_s$ specimen) and the size of its elements (COD $\approx 2\mu m$ when the specimen is unloaded). Those experiments will also allow to assess the effect of the interactions between damage of consecutive plies.

ACKNOWLEDGEMENTS

REFERENCES

[1] P. Ladevèze and G. Lubineau. Relationships between 'micro' and 'meso' mechanics of laminated composites. *Compte Rendu Mécanique*, 331(8):537–544, 2003.

[2] Cédric Huchette. *Sur la complémentarité des approches expérimentales et numériques pour la*

modélisation des mécanismes d'endommagement des composites stratifiés. Phd thesis, Université Paris 6, France, 2005.

[3] Jean-Charles Malenfant. *Étude de l'influence de l'endommagement sur la perméabilité des matériaux composites, application à la réalisation d'un réservoir cryogénique sans liner*. PhD thesis, Université Bordeaux I, 2012.

[4] Christophe Bois, Jean-Charles Malenfant, Jean-Christophe Wahl, and Michel Danis. A multi-scale damage and crack opening model for the prediction of flow path in laminated composite. *Composites Science and Technology*, 97:81–89, 2014.

[5] A. Parvizi, K.W. Garrett, and J.E. Bailey. Constrained cracking in glass fibre-reinforced epoxy cross-ply laminates. *Journal of Materials Science*, 13(1):195–201, January 1978.

[6] Peter Gudmundson and Johan Alpman. Initiation and growth criteria for transverse matrix cracks in composite laminates. *Composites Science and Technology*, 60(2):185–195, February 2000.

[7] Dominique Leguillon. Strength or toughness? A criterion for crack onset at a notch. *European Journal of Mechanics - A/Solids*, 21(1):61–72, January 2002.

[8] John A. Nairn. Matrix microcracking in composites. In *Comprehensive composite materials. Vol.2, Polymer matrix composites*, volume 2, pages 403–432. Elsevier, 2000.

[9] Nicolas Tual, Nicolas Carrère, and Malick Diakhaté. Multiscale model based on a finite fracture approach for the prediction of damage in laminate composites. In *ICCM19*, Montréal, Canada, July 2013.

[10] Hortense Laeuffer, Brice Guiot, Jean-Christophe Wahl, Nicolas Perry, Florian Lavelle, and Christophe Bois. A model for the prediction of transverse crack and delamination density based on a strength and fracture mechanics probabilistic approach. In *ECCM17*, Munich, Germany, June 2016.